Honors Theses at the University of Iowa

Spring 2018

Finding Gravitationally Lensed Systems in the VLA Stripe 82 Survey

Jacob Isbell
University of Iowa

FINDING GRAVITATIONALLY LENSED SYSTEMS IN THE VLA STRIPE 82 SURVEY

by

Jacob Isbell

A thesis submitted in partial fulfillment of the requirements
for graduation with Honors in the Astronomy

_____
Hai Fu
Thesis Mentor

Spring 2018

All requirements for graduation with Honors in the
Astronomy have been completed.

_____
Cornelia Lang
Astronomy Honors Advisor

Finding Gravitationally Lensed Systems in the VLA Stripe 82 Survey

Jacob W. Isbell, Hai Fu

May 9, 2018

Abstract

We describe the selection, observations, and analysis of four potential gravitationally lensed radio active galactic nuclei within the VLA Stripe 82 Survey. Using the Very Large Array, we have obtained high-resolution ($0.3''$) observations of two of the four candidates. We analyze the source morphology and 5-7GHz spectral index of each source to determine whether the sources are indeed lensed. We find that neither of the observed sources are lensed, and instead they are core-jet systems contained within the host galaxies. The radio complexes at 00:42:31.4-00:43:40.6 and 01:24:55.9+00:11:17.4 are compact and extend 16.2 kpc and 19.4 kpc respectively. We also find compact, unresolved radio cores with flat spectral indices ($\alpha > -0.12$) at the center of each complex. These systems, while not the lensed systems we sought, can serve as windows into the growth of radio jets and their propagation through the interstellar medium of the host galaxy.

1 Introduction

Gravitational lenses empower astronomers. For the background lensed sources, the flux amplification and the angular magnification enable measurements of the properties of distant galaxies to levels otherwise unattainable with current instrumentation (e.g., Stark et al., 2008; Swinbank et al., 2011; Fu et al., 2012; Dye et al., 2015). For the foreground lensing sources, the geometry and flux distribution of lensed images offer direct measurements of the total dark+baryon mass within the Einstein radius (e.g., Bolton et al., 2007). When quasars are strongly lensed, time-delay measurements allow determinations of the Hubble constant (Refsdal, 1964; Treu & Marshall, 2016; Bonvin et al., 2017), and absorption-line spectroscopy probes the chemical composition of the foreground interstellar medium (e.g., Wiklind & Combes, 1996; Muller et al., 2016). However, strongly lensed systems are rare: e.g., the HST Snapshot survey of 502 luminous quasars detected only five lens systems (Bahcall et al., 1992; Maoz et al., 1993). Therefore, efficient methods to identify strong lenses are desirable (e.g., Bolton et al., 2006; Jackson & Browne, 2007; Negrello et al., 2010). Here we describe such a method to identify strongly lensed radio AGNs with spatially resolved spectral slope measurements.

The spectral slopes of extragalactic radio sources in GHz frequencies correlate well with their morphologies. Flat-spectrum sources ($\alpha > -0.5$, where $S_\nu \propto \nu^\alpha$) are dominated by compact milliarcsec-scale radio cores in the nuclei of radio galaxies. Steep-spectrum sources ($\alpha < -0.5$) are dominated by complex extended structures over a range of sizes. Therefore, a flat-spectrum source is not expected to show multiple components unless it is strongly lensed. Indeed, the first flat-spectrum radio source known to show an arcsec-scale double structure is the famous lensed quasar PKS 1830−211 at $z = 2.507$ (Pramesh Rao & Subrahmanyan, 1988; Nair et al., 1993; Wiklind & Combes, 1996). Furthermore, previous Very Large Array (VLA)-based strong lens surveys have

focused on flat-spectrum sources to avoid confusion between lensed morphologies and intrinsically complex morphologies: e.g., the Jodrell Bank VLA Astrometric Survey (JVAS; King et al., 1999), the Cosmic Lens All-Sky Survey (CLASS; Myers et al., 2003; Browne et al., 2003), and the Southern VLA-based Gravitational Lens Search (Winn et al., 2001). In particular, JVAS and CLASS imaged 11,685 flat-spectrum sources brighter than $S_{\mathrm{5GHz}} > 30$ mJy with the VLA at 8 GHz in the A-configuration and identified 22 strong lenses. Although the surveys provided a statistical sample well suited for lens statistics, the $\sim 0.2\%$ efficiency of the method can be significantly improved if additional data can be used to weed out the majority of the contaminants: flat-spectrum sources that do not show multiple peaks and/or potential lensing galaxies in deep optical images.

By exploiting multi-frequency arcsec-resolution VLA surveys covering 92 deg^2 of the Stripe 82 field, we have identified a sample of flat-spectrum sources with arcsec-scale double structures (Fig. 1). The sources are selected to show semi-symmetric morphologies with respect to an optical source in the SDSS deep coadds. Here we utilize VLA A-configuration C-band imaging to confirm these strong candidate lensed sources. With the new $0.3''$ deep radio images, we will test the lensing hypothesis using the following expected observational signatures of lensing: (1) symmetric 5-7GHz spectral slope variations, (2) consistent surface brightness distributions in the lensed images, and (3) diffuse Einstein-ring-like substructures. For promising candidates, lens models will be built to test if lensing is feasible to create the observed morphologies.

This paper is organized as follows: In §2 we outline the sample selection; in §3 we discuss the VLA observations. In §4 we analyze and discuss the new data, and in §5 we summarize our results. Throughout we adopt the ΛCDM cosmology with $\Omega_m = 0.27$, $\Omega_\Lambda = 0.73$, and $h = 0.7$.

2   Sample Selection

To compile a sample of flat-spectrum radio galaxies with double structures, we select arcsec-separation double radio sources from the part of the SDSS Stripe 82 field that have arcsec-resolution VLA images. The 92 deg^2 field has 1.4 GHz maps (rms ~ 52 μJy/bm) from the VLA Survey of Stripe 82 (VS82; Hodge et al., 2011) and 5-epoch-coadded 3.0 GHz maps (rms ~ 40 μJy/bm) from the Caltech-NRAO Stripe 82 Survey (CNSS; Mooley et al., 2016). The Stripe 82 field has been repeatedly scanned $70-90$ times in the $ugriz$ bands by the SDSS imaging survey. The 5σ detection limit of the deep coadds is 24.6 AB in r-band, about 2 magnitudes deeper than the best SDSS single-epoch images. We begin by matching the VS82 1.4 GHz source catalog with the optical r-band catalog from the depth-optimized Stripe 82 coadds (Jiang et al., 2014) with a matching radius of $3''$. We then find that 261 r-band sources are associated with two radio sources within the matching radius. Finally, we restrict the sample to the 62 radio pairs that show good symmetry around the optical source ("symmetric doubles" hereafter). Specifically, we require (1) the optical source is brighter than $r < 23$, (2) the sources in each radio pair have comparable flux densities ($0.5 \leq S1/S2 \leq 2.0$) and comparable offsets from the optical source ($0.5 \leq \mathrm{Sep}_1/\mathrm{Sep}_2 \leq 2.0$), and (4) the offset between the central position of the radio pair and the optical source is less than 20% of the pair separation. Note that our sample selection is quite conservative because of these strict requirements. For comparison, the CLASS survey included all of the sources that show component flux density ratios greater than 1:10 (Browne et al., 2003).

Most of the 62 symmetric doubles are probably radio lobes generated by the AGN in the optical galaxy, i.e., FR II type radio galaxies. To remove those, we use spectral slope measurements. We generate 3 GHz cutout images for the 62 symmetric doubles using the CNSS data. The calibrated data were imaged using the CLEAN task with a circular $1.8''$ beam and $0.6''$ pixels to match the VS82 1.4 GHz images. We calculate the two-frequency spectral slope maps using the matched-resolution
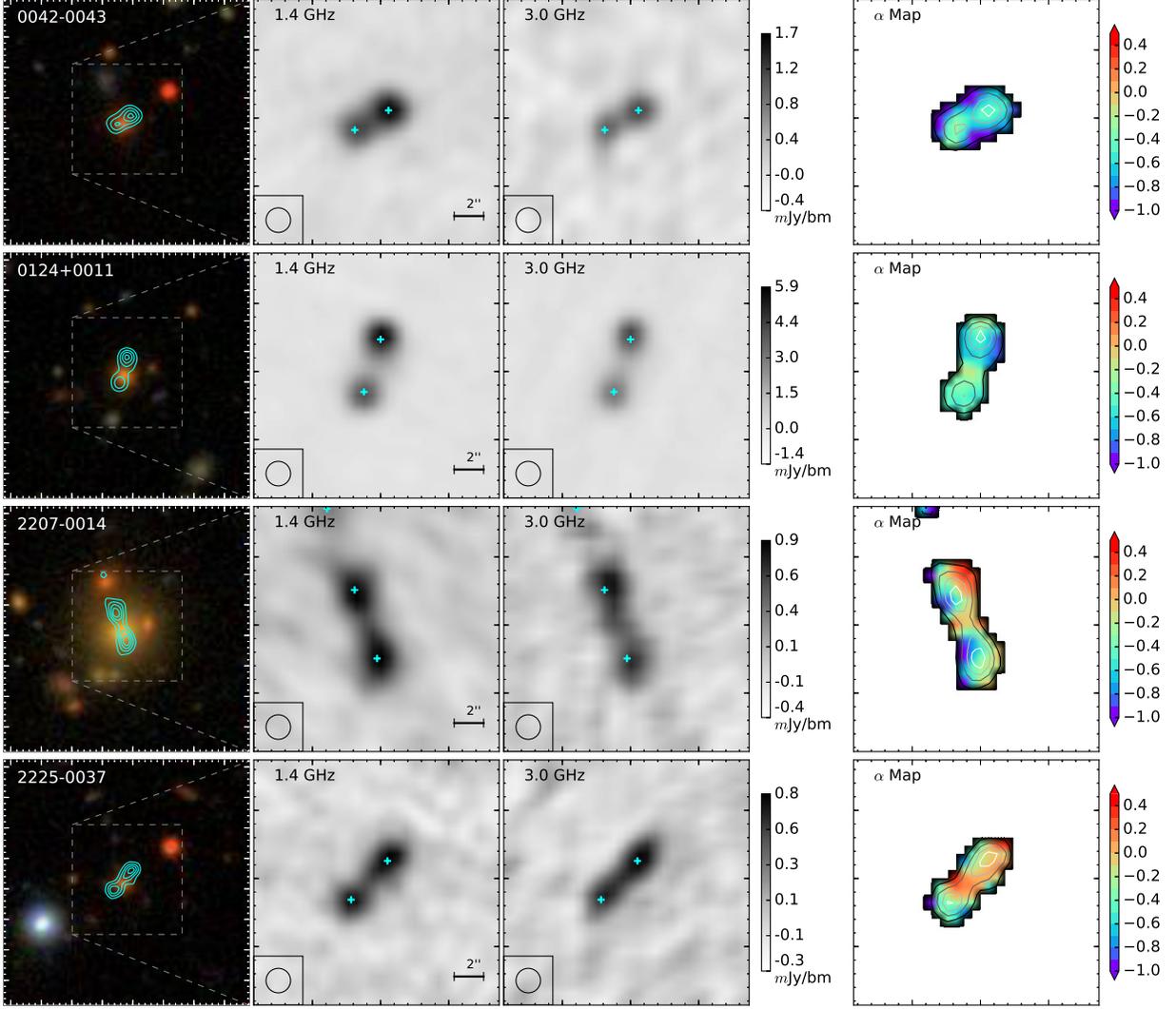
Figure 1: Our proposed targets: Flat-spectrum radio sources with double structures. For each system we show (from left to right): a wide-field SDSS Stripe 82 coadded gri color image overlaid with contours showing the 1.4 GHz continuum map from VS82 (Hodge et al., 2011), the 1.4 GHz VLA map from VS82, the 3.0 GHz VLA map from the Caltech-NRAO Stripe 82 Survey (CNSS; Mooley et al., 2016), and the 1.4-3 GHz spectral index map ($S \propto \nu^{\alpha}$). The contours start at 2σ and continue exponentially to the peak value of the 1.4 GHz map. Crosses mark the VS82 catalog source positions.

1.4 GHz and 3 GHz images and measure the spectral slope for each source using the peak flux densities. We calculate the uncertainty of the spectral slope measurements based on the SNRs of the sources in each frequency. Roughly speaking, $\delta\alpha \sim 0.2$ when SNR = 10 in both frequencies. In Fig. 2, we show the spectral slope vs. flux density for all of the sources in the symmetric doubles. As expected, the α distribution is peaked at -0.7, the typical value for extragalactic sources (e.g., Smolčić et al., 2017). Given the large uncertainties at low flux densities, we consider a source flat-spectrum only when the measured α value is more than 1.5σ away from the $\alpha = -0.5$ dividing line between flat-spectrum and steep-spectrum sources; i.e., $(\alpha - 1.5\delta\alpha) > -0.5$. We also exclude the sources with 1.4 GHz peak flux densities less than 0.6 mJy/bm because of their low S/N. We find a total of 11 flat-spectrum sources out of the 124 sources. Three of the flat-spectrum sources are in pairs where the other source shows a steep spectrum. The remaining eight flat-spectrum
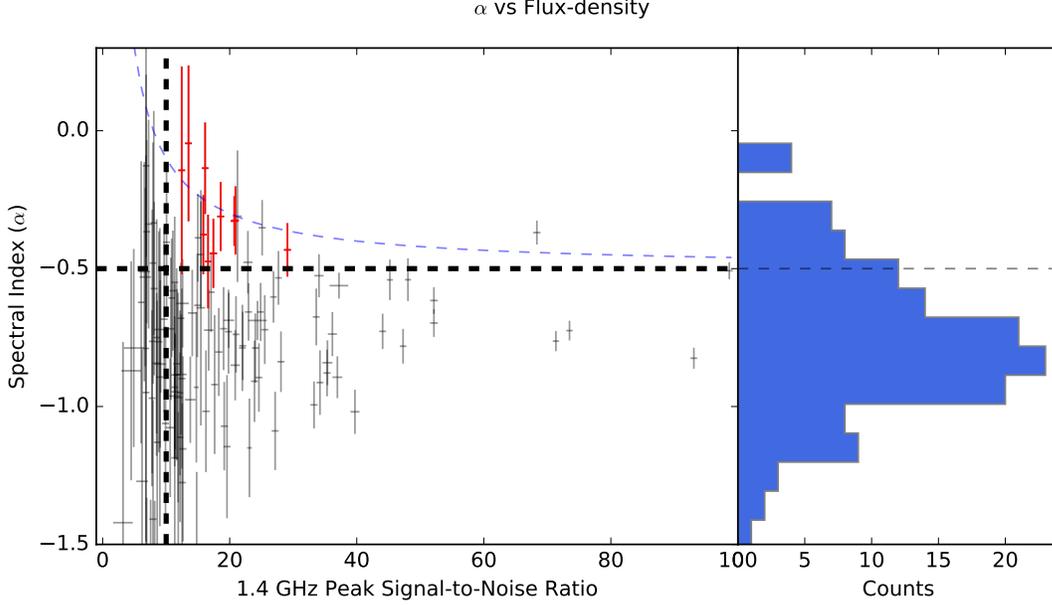
α vs Flux-density

Figure 2: Our target selection. The left panel shows the spectral slope (α) vs the 1.4 GHz peak signal to noise ratio for 124 sources in our 62 candidate fields. The right panel shows the α distributions for all sources with $\mathrm{SNR_{1.4GHz}} > 10$. The horizontal dashed line at $\alpha = -0.5$ marks the division between flat-spectrum and steep-spectrum sources. The vertical dashed line marks the SNR= 10 division. The dashed blue line indicates "ideal" uncertainty in spectral slope $\sigma \propto 1/\mathrm{SNR}^2$. Red crosses indicate the components of each of the 4 candidates.

sources in four symmetric pairs form our final sample (see Fig. 1 and Table 1).

Based on existing data, all four sources are consistent with the strong lensing interpretation. First, the components in each pair show spectral slopes that are consistent within the uncertainties, so they could be lensed images of the same source. The 3-5$''$ separations between the radio sources and the redshifts of the optical galaxies ($0.23 < z < 0.54$) are also consistent with the expected size of the Einstein radius (θ_E) of massive galaxies: $\theta_E = 2.596"(\sigma/300\mathrm{kms}^{-1})^2 D_{\mathrm{LS}}/D_{\mathrm{S}}$, where σ is the stellar velocity dispersion (assuming a singular isothermal ellipsoid density profile) and D_{LS} and D_{S} are the angular diameter distances between the lens and the source and between the source and the observer, respectively. Existing optical and near-IR data are not deep enough to detect the host galaxies of the lensed radio sources, which are likely at high redshifts.

Table 1: VLA- Observed Targets for 2018A: Double Flat-Spectrum Sources in Stripe 82

Coordinates	Desig	z	$S_{peak}^{1.4GHz}$ (mJy/bm)	$S_{peak}^{3.0GHz}$ (mJy/bm)	$\alpha_{1.4-3GHz}$
00:42:31.438-00:43:40.620	0042-0043	0.549	1.60±0.05	1.19±0.08	-0.38±0.10
00:42:31.603-00:43:42.060	0042-0043	0.549	1.15±0.05	0.96±0.08	-0.23±0.12
01:24:55.946+00:11:17.350	0124+0011	0.467	5.67±0.06	4.14±0.09	-0.41±0.03
01:24:56.027+00:11:13.490	0124+0011	0.467	3.93±0.06	2.96±0.09	-0.37±0.04
22:07:15.461-00:14:53.350	2207-0014	0.231	0.84±0.05	0.70±0.08	-0.23±0.17
22:07:15.351-00:14:58.380	2207-0014	0.231	0.86±0.05	0.67±0.08	-0.32±0.17
22:25:41.517-00:37:00.220	2225-0037	0.537	0.72±0.05	0.72±0.15	-0.00±0.28
22:25:41.695-00:37:03.070	2225-0037	0.537	0.67±0.05	0.53±0.15	-0.30±0.38

Notes: The two sources in bold have been observed as of the writing of this thesis.

3   Observations

We were awarded 2.6 hrs of Very Large Array (VLA) observing time split into a block of B-priority and a block of C-priority. (At this time) we observed 2 of 4 gravitational lens candidates in A configuration with C-band receivers [1]. The receivers have a central frequency of 5.9985 GHz and a bandwidth of 4 GHz. We grouped the candidates into two scheduling blocks (SBs) of 1.3hrs each. The sources were grouped by their RA (one SB had RA ~ 0 hr, the other RA~ 23 hr). At the beginning of each SB, 3C48 was observed for flux-density and bandpass calibrations.

The observations were calibrated using the Common Astronomical Software Applications (CASA) package. We used the VLA pipeline to perform the basic calibration and data flagging. Upon inspection of the data quality, we decided further flagging would be unnecessary. We used a self-calibration technique to improve the calibration derived from the calibrator 0125-0005. For beam deconvolution and imaging we employed the CASA task CLEAN; we used a Briggs robust parameter of 0.5 to improve image fidelity with only a mild loss of sensitivity relative to "natural" weighting. The resulting restored beams are on average $0.32'' \times 0.32''$ in FWHM. We used a pixel size of $0.1''$ to sample the restoring beam with ~ 3 pixels. We ran the iterative cleaning process until the rms noise of the field dropped below $3\times$ the expected radiometer noise (4μJy beam^{-1}). To model the frequency dependence on source flux density (i.e. the spectral slope α), we adopt two Taylor terms with CLEAN, and take the ratio of the first two terms in areas of sufficient signal-to-noise ratio (Rau & Cornwell, 2011).

4   Analysis and Results

We examine the morphology, spectral slope, and surface brightness of each source to determine if it is a lensed system. We also compare the new high-resolution maps to the 1.4 GHz survey maps to understand how features correspond. A lensed system will exhibit (1) similar morphologies about the foreground, lensing galaxy; (2) symmetric variations in the spectral slope (5-7 GHz); (3) diffuse substructures akin to Einstein rings.

4.1   Morphology

In Figure 3 we show the high-resolution radio maps with contours. Visual inspection immediately indicates roughly symmetric surface brightness distributions about the centers. In both fields, however, we find a bright point source between the "lobes". Because the point source is unresolved, it cannot be a foreground galaxy. Instead it is most likely a compact radio core (i.e. an AGN) driving the symmetric jets previously observed as point sources.

These objects are quite compact. 0042-0043 has jets with a maximum extent of merely 16.2 kpc ($2.5''$ at $z = 0.549$) from the core. 0124+0011 has an extent of 19.4 kpc ($3.2''$ at $z = 0.467$). These distances are measured from the center of the unresolved point source to the farthest 2σ emission. The jet sizes are on the order the size of the host galaxy (~ 15-25 kpc), and thus are very compact compared to a proto-typical FR-II, 3C 175, which has jets 200 kpc long (Fernini, 2007).

We find no evidence of Einstein-ring-like diffuse substructures in either source. These structures would be seen as arcs around the central lensing mass (e.g. Nair et al. (1993)). We find essentially no signal (above 2σ) away from the major axis of emission, further supporting the jet hypothesis rather than a strong lensing scenario.

---

[1]Program 18A-195 (PI: Isbell)

4.2 Spectral Slope

We compute the 5-7 GHz spectral slope using two Taylor expansion terms in the CASA CLEAN function. The ratio between the first two terms gives the spectral slope α at each pixel, building an α-map. In each field we assess three objects: (A) the unresolved point source near the center of emission; (B) the northern jet, with position given from the 1.4 GHz catalog (Hodge et al., 2011); and (C) the southern jet with position defined the same way. For the jets we compute the average spectral slope by taking a flux-weighted mean within a 6 px circle ($2 \times$ the beam FWHM) centered on the source. The unresolved point source is measured within one beam FWHM as to avoid the surrounding emission. These results are listed in Table 2. Errors at each pixel are calculated by comparing the measured flux to a predicted flux from the assumed pixel α and the frequency range to each spectral window (Rau & Cornwell, 2011).

In all the jets, we find $\alpha < -0.7$ which is consistent with compact steep spectrum (CSS) sources (O'Dea, 1998). In the cores, however, we measure a much shallower $\alpha \simeq -0.1$. Our search for lensed AGN was based on the hypothesis that a radio core would exhibit a flat or inverted spectral slope due to synchrotron self-absorption ($\alpha \to 5/2$ for a homogenous source), and this is confirmed. The steep slopes of the jets approach the spectral index expected from synchrotron emission above the turnover frequency ($\alpha = -0.7$), but inhomogeneities in morphology (i.e. lobes, hot spots, etc.) may alter the slope (O'Dea (1998); Laing et al. (2006)).

As a final check of whether or not these are lensed sources, we compare the spectral slopes of the northern and southern components. If we are indeed observing a lensed AGN, the spectral variations should be symmetric about the central source. In 0042-0043 the spectral slopes of the components are the equal (within errors), but the large uncertainty in the slope measurements in addition to the extended, asymmetric morphology make a lensing scenario unlikely. The components of 0124+0011 have much higher flux densities, so the uncertainty in α is much smaller. The northern and southern component slopes vary by $\sim 1\sigma$.

5 Discussion

Neither of the observed sources exhibit the characteristics of gravitationally lensed AGN; they do not have Einstein-ring substructures, symmetric spectral variations, or symmetric surface brightness distributions around the lensing mass. While 0042-0043 has symmetric α values, the large uncertainties and overall morphology make the lensing scenario unlikely. We find a flat-spectrum core (likely an accreting SMBH) at the center of the jet structure. The compact size of the jet-core complex suggests it is contained wholly within the host galaxy. The surface brightness of 0124+0011 is very asymmetric – the northern component has a peak flux density of $\sim 900\mu$Jy bm^{-1}, while the southern has only 160μJy bm^{-1}. If these are indeed jets, this is likely a result of relativistic beaming of the synchrotron emission (Laing et al., 2006). Each jet extends only 19.4 kpc from the core, and this complex is also contained within the host galaxy.

Both observed candidates closely resemble CSS galaxies. CSS sources reside entirely within the host galaxy (jet scales ≤ 20 kpc) and exhibit steep radio spectral slopes above ~ 1 GHz. They are closely related to Gigahertz Peaked Spectra (GPS) sources, which exhibit slightly flatter spectra, longer electron lifetimes, and are often embedded within the CSS. They both have turnovers in their radio spectra which give insight into the physical properties and host environments of the source (O'Dea, 1998). Evidence suggests that CSS/GPS sources are the progenitors of "large" radio AGN such as FR-IIs (Carvalho (1985); Readhead et al. (1996); Mutel & Phillips (1988)). The spectral index and size measurements of 0042-0043 and 0124+0011 indicate that our lensing candidates are
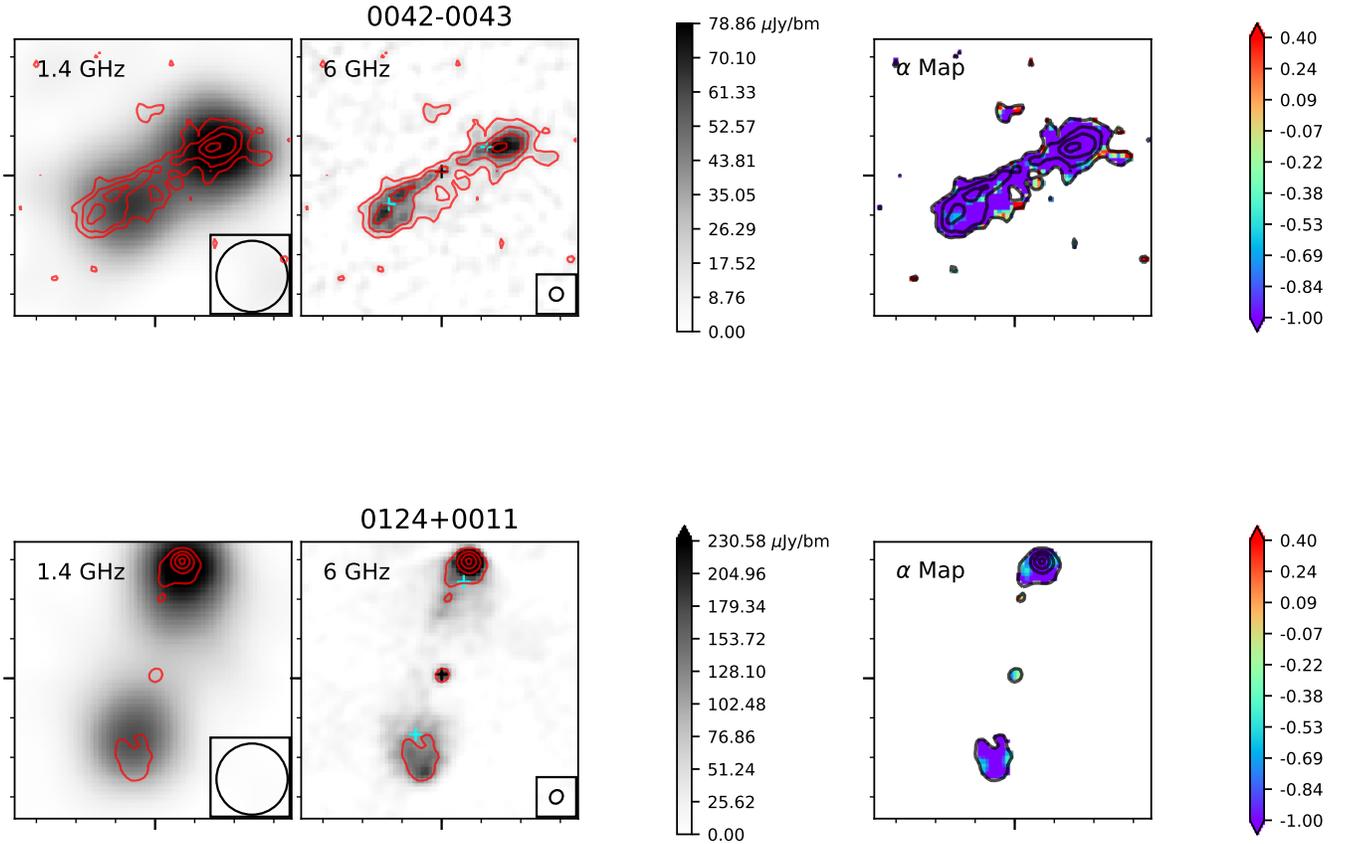
Figure 3: In each row we present (left) the 1.4 GHz radio map from Hodge et al. (2011); (center) the high-resolution VLA *C*-band map; and (right) the spectral index (5-7 GHz) map. In each case we overplot the *C*-band contours beginning at 2σ and continuing exponentially to the peak flux density. Cyan crosses are the Hodge et al. (2011) catalog source positions. The black cross marks the compact radio core found in each image. Major ticks indicate $5''$ and minor ticks indicate $1''$.

instead CSS pairs which we have resolved into jets and a luminous central core. The previous spectral slope measurements from 1.4 GHz to 3 GHz must have occurred near the "turnover" in the spectral energy distribution, leading to our misidentification of jets as accreting SMBHs.

The radio cores, however, exhibit flat or inverted spectra in the same frequency range. This indicates that we are observing them below the critical (or turnover) frequency,

$$\nu_c \sim \frac{\gamma^2 eB}{2\pi m_e c} \tag{1}$$

where B is the magnetic field strength of the region and γ is the Lorentz factor of an electron emitting at frequency ν. Below the cutoff frequency, synchrotron self-absorption by relativistic electrons will cause $S \propto \nu^{5/2}$ (O'Dea, 1998). The radio cores of 0042-0043 and 0124+0011 have peak flux densities at 6 GHz of 21.3 ± 13.3 μJy bm^{-1} and 201.9 ± 53.4 μJy bm^{-1} respectively. Because the core of 0042-0043 exhibits a negative slope at 6 GHz, we infer that it has turned over. If we use 6 GHz as the turnover frequency (the slope is ~ 0 within errors) and assume a synchrotron

Table 2: Spectral slope values (5-7 GHz) for each component of the resolved lensing candidates.

Designation	North Jet α	South Jet α	Core α
0042-0043	-1.41 ± 0.90	-1.49 ± 0.70	-0.12 ± 0.82
0124+0011	-0.69 ± 0.15	-0.42 ± 0.23	-0.16 ± 0.17

self absorption slope of $\alpha = 5/2$ at lower frequencies, then at 1.4 GHz this source would have a peak flux density of 0.56 μJy bm^{-1} – well below the 52 μJy bm^{-1} rms noise of the Hodge et al. (2011) survey. Similarly, if we assume from the near-zero measured slope of 0124+0011's core that it is turning over and set $\alpha = 5/2$, then at 1.4 GHz the peak flux density would be 5.3 μJy bm^{-1}. It is thus unsurprising that these core components were undetected in our initial candidate selection. Even with a conservative $\alpha = 1$ (because $\alpha = 5/2$ is rarely observed due to inhomogeneities in morphology), the brighter source 0124+0011 would have $S_{peak,core} \approx 47$ μJy bm^{-1}, still below the rms noise of the previous survey.

Our selection methods were based on the synchrotron self-absorption-driven spectral energy distribution of high-density regions near a galaxy's accreting SMBH. 1.4 GHz is near the expected turnover frequency of these systems, but we find that these young jets are optically thick enough to exhibit the same SED. The compact radio cores at the center of each map have flat or inverted spectral slopes even at 6 GHz. The higher angular resolution of a given configuration at 6 GHz compared to 1.4 or 3 GHz, as well as the "late" peaking compact cores of this sample suggest that the same selection methods with $\alpha_{1.4-3} \rightarrow \alpha_{5-7}$ would be better suited to identifying strongly lensed AGN. Additionally, the ongoing VLA Sky Survey at 2-4 GHz with a rms per epoch of 120μJy bm^{-1} and 2.5$''$ resolution can provide provide a comparable, but much larger, strongly lensed candidate sample to this work (Lacy et al., 2016).

6 Conclusions

We present two VLA C-band radio maps of candidate strongly lensed AGN. Based on the surface brightness distributions, spectral slope measurements, and lack of Einstein-ring substructures, we conclude that neither observed candidate is a lensed AGN. Instead, they are similar in morphology to FR-II galaxies. These radio complexes reside within their host galaxies, and should be classified as CSS sources. While they cannot be used to study cosmological parameters as per a set of strongly lensed sources, these galaxies provide an opportunity to study the evolution of radio AGN. The observed jets are still pushing against the host's interstellar medium, and thus are prime location to study the host's magnetic field and composition. These jets will produce shock fronts, and X-Ray observations can yield insights into their temperatures, lifetimes, and propagation (Heinz et al., 1998). While our search for strongly lensed AGN has failed, we have identified two evolving jet-core complexes for further study at high redshift.

References

Bahcall, J. N., Maoz, D., Doxsey, R., et al. 1992, ApJ, 387, 56

Bolton, A. S., Burles, S., Koopmans, L. V. E., Treu, T., & Moustakas, L. A. 2006, ApJ, 638, 703

Bolton, A. S., Burles, S., Treu, T., Koopmans, L. V. E., & Moustakas, L. A. 2007, ApJ, 665, L105

Bonvin, V., Courbin, F., Suyu, S. H., et al. 2017, MNRAS, 465, 4914

Browne, I. W. A., Wilkinson, P. N., Jackson, N. J. F., et al. 2003, MNRAS, 341, 13

Carvalho, J. C. 1985, MNRAS, 215, 463

Dye, S., Furlanetto, C., Swinbank, A. M., et al. 2015, ArXiv e-prints

Fernini, I. 2007, AJ, 134, 158

Fu, H., Jullo, E., Cooray, A., et al. 2012, ApJ, 753, 134

Heinz, S., Reynolds, C. S., & Begelman, M. C. 1998, ApJ, 501, 126

Hodge, J. A., Becker, R. H., White, R. L., Richards, G. T., & Zeimann, G. R. 2011, AJ, 142, 3

Jackson, N., & Browne, I. W. A. 2007, MNRAS, 374, 168

Jiang, L., Fan, X., Bian, F., et al. 2014, ApJS, 213, 12

King, L. J., Browne, I. W. A., Marlow, D. R., Patnaik, A. R., & Wilkinson, P. N. 1999, MNRAS, 307, 225

Lacy, M., Baum, S. A., Chandler, C. J., et al. 2016, in American Astronomical Society Meeting Abstracts, Vol. 227, American Astronomical Society Meeting Abstracts #227, 324.09

Laing, R. A., Canvin, J. R., Bridle, A. H., & Hardcastle, M. J. 2006, MNRAS, 372, 510

Maoz, D., Bahcall, J. N., Schneider, D. P., et al. 1993, ApJ, 409, 28

Mooley, K. P., Hallinan, G., Bourke, S., et al. 2016, ApJ, 818, 105

Muller, S., Müller, H. S. P., Black, J. H., et al. 2016, A&A, 595, A128

Mutel, R. L., & Phillips, R. B. 1988, in IAU Symposium, Vol. 129, The Impact of VLBI on Astrophysics and Geophysics, ed. M. J. Reid & J. M. Moran, 73

Myers, S. T., Jackson, N. J., Browne, I. W. A., et al. 2003, MNRAS, 341, 1

Nair, S., Narasimha, D., & Rao, A. P. 1993, ApJ, 407, 46

Negrello, M., Hopwood, R., De Zotti, G., et al. 2010, Science, 330, 800

O'Dea, C. P. 1998, PASP, 110, 493

Pramesh Rao, A., & Subrahmanyan, R. 1988, MNRAS, 231, 229

Rau, U., & Cornwell, T. J. 2011, A&A, 532, A71

Readhead, A. C. S., Taylor, G. B., Xu, W., et al. 1996, ApJ, 460, 612

Refsdal, S. 1964, MNRAS, 128, 307

Smolčić, V., Novak, M., Bondi, M., et al. 2017, A&A, 602, A1

Stark, D. P., Swinbank, A. M., Ellis, R. S., et al. 2008, Nature, 455, 775

Swinbank, A. M., Papadopoulos, P. P., Cox, P., et al. 2011, ApJ, 742, 11

Treu, T., & Marshall, P. J. 2016, A&A Rev., 24, 11

Wiklind, T., & Combes, F. 1996, Nature, 379, 139

Winn, J. N., Hewitt, J. N., & Schechter, P. L. 2001, in Astronomical Society of the Pacific Conference Series, Vol. 237, Gravitational Lensing: Recent Progress and Future Go, ed. T. G. Brainerd & C. S. Kochanek, 61